



LESSONS LEARNED FOR LIFELINE ENGINEERING FROM MAJOR URBAN EARTHQUAKES

T.D. O'ROURKE

School of Civil and Environmental Engineering, Cornell University, Ithaca, NY 14853

ABSTRACT

This paper reviews the performance of lifelines during the 1989 Loma Prieta ($M_w = 6.9$), 1994 Northridge ($M_w = 6.7$), and 1995 Hyogoken-Nanbu ($M_w = 6.9$) earthquakes. The interaction among different lifeline systems is described. Buried pipeline response to transient motion is discussed, and a simplified procedure is proposed for assessing damage potential by means of seismic response diagrams. The amplification of transient motion at liquefaction sites is discussed. Long period transient displacements at liquefaction sites are shown to be a cause of water distribution piping failure during the 1989 Loma Prieta earthquake, and procedures are proposed for identifying and quantifying this hazard. Construction procedures for reducing the effects of permanent ground deformation on buried pipelines are summarized. A special "frictionless" wrap is described that reduces substantially the longitudinal friction between pipe and surrounding soil, thereby allowing the pipeline to accommodate additional movement at fault crossings and landslides. Geographical information systems and real time monitoring are described in relation to lifeline system management and emergency response planning.

KEYWORDS

Electric power, fault crossings, gas and liquid fuels, lifeline earthquake engineering, liquefaction, near source effects, permanent ground deformation, pipeline coating, pipelines, site response, telecommunications, transient ground motion, transportation, wastewater facilities, water supply.

INTRODUCTION

The performance of lifelines during the 1989 Loma Prieta ($M_w = 6.9$), 1994 Northridge ($M_w = 6.7$), and 1995 Hyogoken-Nanbu ($M_w = 6.9$) earthquakes is discussed in this paper. Each earthquake was of moderate magnitude, but was located near a highly populated, urban center with high densities of transportation infrastructure, water supply and wastewater facilities, gas and liquid fuel lines, telecommunications, and electric power system components. The salient features of the seismic performance of each lifeline system are summarized for each earthquake. Comparisons are made among the earthquakes, and the interdependencies among different systems are discussed. A simplified procedure for evaluating buried pipeline response to transient ground motion is introduced in the form of a seismic response diagram that identifies the predominant period, peak particle velocity, and wave propagation velocity necessary to cause damage. The procedure is shown to predict correctly the damage sustained by large diameter water

transmission lines during the 1985 Michoacan and 1994 Northridge earthquakes. Research findings associated with buried pipeline response to transient motion at liquefaction sites are summarized. Large transient shear strains and long period displacements are shown to be the primary cause of damage to water distribution piping in the Marina of San Francisco during the 1989 Loma Prieta earthquake. Methods of reducing shear resistance between pipe and soil are discussed as a means of constructing or retrofitting pipelines to accommodate additional permanent ground displacement at fault crossings and landslide sites. A description is provided of a special "frictionless" wrap, which is composed of easily installed geosynthetics, to reduce substantially the longitudinal friction between pipe and surrounding soil. The paper finishes with a discussion of future trends in lifeline system management and emergency response by means of geographical information systems(GIS) and real time monitoring.

EARTHQUAKE PERFORMANCE OF LIFELINES

Lifelines are a distinguishing characteristic of modern communities, providing the services and resources necessary for security, commerce, and communications. When earthquakes strike urban centers, they disrupt lifeline systems, threatening life and property in the short term and prolonging economic recovery during post earthquake construction and rehabilitation. The 1985 Michoacan earthquake was one of the first severe earthquakes to affect a modern conurbation with complex transportation, telecommunication, water supply, and power systems. Since the destructive consequences of this earthquake in Mexico City, there have been three major earthquakes that have struck modern urban centers in North American and Japan: the 1989 Loma Prieta, 1994 Northridge, and 1995 Hyogoken-Nanbu earthquakes.

Tables 1 and 2 provide a summary of the salient features of these earthquakes with respect to lifeline systems. For each earthquake, the response of water supplies, gas and liquid fuel lines, transportation networks, electric power systems, telecommunications, and wastewater facilities are described briefly. Because lifelines cover large geographical areas and are composed of many diverse components, it is helpful to develop a view of large-scale effects, such as provided in the table. In this way, similarities in lifeline performance during different earthquakes can be perceived, vulnerable features can be identified, and the interaction among different systems in emergency conditions can be better understood.

Lifeline Interaction With Electric Power

A review of the lifeline performance summarized in the tables reveals that electric power systems generally have performed well. Restoration for the great majority of customers who lost service has required one to two days. Electric power restoration after the 1995 Hyogoken-Nanbu earthquake required a relatively long time compared with power systems affected by other recent earthquakes (UNCRD, 1995). In the Kobe area, many utility poles were damaged by collapsed buildings, and some underground cables required several days for repair. Although system restoration has been rapid, the scale of the outages has been very large, affecting more than 1 million customer locations in each of the earthquakes considered.

Another observation about lifeline performance is that electric power is critically important for other lifelines, with power loss reflected directly in reduced serviceability of water supplies, wastewater facilities, telecommunications, and transportation. There are many examples of electric power effects, including loss of sewage and water pumping capacity in all three earthquakes, loss of rapid transit services during the Loma Prieta earthquake, and loss of power for phone service during the Northridge and Hyogoken-Nanbu earthquakes. Even though power losses are short-lived, their consequences can be quite profound. An important strategy for integrated lifeline management is to focus on electric power reliability and to implement procedures for rapid restoration.

The restoration of electric service, however, needs to be coordinated carefully with the restoration of potential hazardous lifelines. Figure 1 shows the restoration plot for the Kansai Electric Power Company after the Hyogoken-Nanbu earthquake. There is a noticeable increase in customers without power about

Table 1. Summary of earthquake effects on lifeline systems: water supply, gas and liquid fuel, and transportation

Earthquake	Water Supply	Gas and Liquid Fuel	Transportation
1989 Loma Prieta $M_w = 6.9$ Maximum MMI = IX Principal References: EERI (1990) NRC (1994) McNutt (1990)	350 main repairs in San Francisco, Oakland, and Berkeley, primarily in 100 to 200-mm cast iron and asbestos cement lines. 240 main repairs in the Santa Cruz area in similar pipelines. Damage concentrated in liquefaction areas. Electric power loss had serious effect on water distribution in San Francisco. Pipeline damage from liquefaction seriously impaired fire fighting in San Francisco.	Only two leaks reported in the transmission system. Over 1000 leaks reported system-wide. Extensive damage to cast iron and steel distribution piping in liquefaction areas such as the Marina in San Francisco and Watsonville. No damage to liquid fuel transmission lines reported. Numerous oil tanks on soft soil sites were damaged.	3 bridges had one or more spans collapse and 10 were closed due to structural damage. The Bay Area Rapid Transit system was virtually undamaged. Airport damage was minor, with the exception of runway closure at Oakland Intl. Airport caused by liquefaction. Port facilities were damaged by liquefaction. Urban transit services were disrupted by electric power loss.
1994 Northridge $M_w = 6.7$ Maximum MMI = IX Principal References: EERI (1995) Schiff (1995)	Over 1400 repairs in Los Angeles distribution system, with nearly 100 repairs in critical large diameter transmission and trunk lines. All three major transmission systems north of San Fernando were disrupted. Performance of dams, wells, and pumping stations was good, although electric power losses caused disruption. Only minor damage to water treatment plants. Significant damage to above-ground tanks constructed according to older design codes.	151,000 gas outages, of which 88% were customer shut-offs. 35 non-corrosion related repairs to transmission lines; 25 at cracked or ruptured oxy-acetylene welds in pre-1932 pipe. Only 27 repairs in polyethylene piping of which 24,000 km were in service. One 1925 petroleum transmission line sustained oxyacetylene weld damage and failures at about 20 locations. No damage in modern transmission lines. Fires at 1 and 2 locations of liquid fuel and gas pipeline damage, respectively. Oil contamination of Santa Clara River from ruptured petroleum line.	Portions of four major highways closed for several months, disrupting traffic and increasing ridership in rail commuter services. Approximately 50% of truck trips to and from Los Angeles were disrupted immediately after the earthquake. Of 1200 bridges experiencing ground accelerations ≥ 0.25 g, 7 sustained severe damage, with an additional 230 requiring moderate to minor repairs. Only minor damage was sustained at port facilities. Minor damage occurred at airports, with little traffic delay.
1995 Hyogoken-Nanbu $M_w = 6.9$ Maximum JMA Intensity = 7 Principal References: NIST (1996) Shinozuka (1995) UNCRD (1995)	1.1 million customer locations lost water. Complete restoration required more than 2.5 months. All 86 reservoirs supplying Kobe City were empty within 24 hrs. Water loss seriously impaired fire fighting. 1610 repairs in distribution mains, and 71,235 repairs in services, caused mostly by building damage and ground deformation. Loss of electric power disrupted pumping in major transmission lines and prevented emergency shut-off valves from working at 3 reservoirs.	857,400 customer locations lost service. Restoration required 3 months. No significant damage to LNG terminals, gas distribution stations, and transmission lines. 106 repairs in medium pressure trunk lines, predominantly at loosened mechanical joints and welds in older steel pipe. 5190 repairs to distribution mains and branches; 10,161 repairs in service lines, and 11,108 repairs of piping attached to buildings. No repairs in polyethylene piping. Good performance reported for seismic shutoff valves.	All railways, highways, and rapid transit systems between Nishinomiya and Kobe were damaged severely. 320 bridges damaged and 9400 roads disrupted. Approximately 27 highway bridges sustained major structural damage. Average automobile traffic counts fell by 50%. Bridge and viaduct performance was influenced by liquefaction-induced lateral spread and site response. Failure of non-ductile reinforced concrete responsible for catastrophic damage.

Table 2. Summary of earthquake effects on lifeline systems: electric power, telecommunications, and wastewater facilities

Earthquake	Electric Power	Telecommunications	Wastewater Facilities
<p>1989 Loma Prieta, $M_w = 6.9$</p> <p>Maximum MMI = IX</p> <p>Principal References: EERI (1990) NRC (1994) McNutt (1990)</p>	<p>1.4 million customers lost power, primarily as a result of damage to transmission sub-stations. Damage was severe in several 500-kV and 230-kV switch yards, with failed live-tank circuit breakers, current transformers, and disconnect switches. Only minor damage at generating stations. Relatively little damage in distribution systems.</p>	<p>Substantial increase in call volume, with 27.8 million calls attempted. Fiber optic cables performed well. Building damage did not disrupt phone service, although damage to a critical telecommunications building in Oakland was substantial and a potentially severe threat to phone service.</p>	<p>Due to power outages and lack of backup power at pumping plants, sewage was released in San Francisco and Monterey Bays. There was extensive damage to sewer mains in liquefaction areas, such as the Marina in San Francisco and Watsonville. Critical, large diameter force mains broke in San Francisco and Santa Cruz. Minor to moderate damage at sewage treatment plants throughout the San Francisco Bay Area.</p>
<p>1994 Northridge, $M_w = 6.7$</p> <p>Maximum MMI = IX</p> <p>Principal References: EERI (1995) Schiff (1995)</p>	<p>Power loss for 1.1 million customer locations plus disruption of 1800 MW power to the northwestern U.S. 93% power restored in 24 hrs. No generating stations in areas of significant strong motion. Damage concentrated in 500-kV and 230-kV substations. Failure of transformer bushings and anchorages, lightning arrestors, disconnect switches, and live-tank circuit breakers. No failures of dead-tank circuit breakers. Transmission towers were damaged by landslides and liquefaction.</p>	<p>Call levels increased above 400% daily averages. Telephone system damage was light to moderate. Structural damage was minor at most central offices. Switch failures resulted in the loss of 3% access lines in Los Angeles. Switch failures and network isolations were most intense in the epicentral area. Most failures related to electric power loss. Fiber optic cables and cellular phone systems performed well.</p>	<p>Minor to moderate damage at sewage treatment plants, mostly from shaking and sloshing in treatment basins. Treatment plant operations were compromised by loss of electric utility power. All 54 sewage booster pumping stations lost electric power in the Los Angeles sewer collection system. Sewer lines were damaged in areas of permanent ground deformation.</p>
<p>1995 Hyogoken-Nanbu $M_w = 6.9$</p> <p>Maximum JMA Intensity = 7</p> <p>Principal References: NIST (1996) Shinozuka (1995) UNCRD (1995)</p>	<p>1 million customers lost service, with 100% restoration within one week after the earthquake. 12 of 35 generating units were shut down, but quickly restored. Five 275-kV and four 77-kV substations were de-energized; damage but no loss of power occurred at 38 additional substations. Transformers, circuit breakers, and power capacitors damaged. Moderate damage to transmission lines and towers. Minor to moderate damage of electric cables in areas of permanent ground deformation.</p>	<p>Call volume increased by a factor of 50. 193,000 lines damaged, of which 100,000 were restored in 2 weeks. 20% telephone lines in Kobe experienced difficulties because of electric power outage. 3 central office buildings sustained damage. Emergency power was disrupted due to loss of water at central offices, losing service to 285,000 lines. Fiber optic cables performed well, even at locations of large permanent ground deformation.</p>	<p>3 of 8 wastewater treatment plants damaged. The Higashi-mada Plant, which is Kobe's largest, was heavily damaged by permanent ground deformation caused by liquefaction. Restoration required more than 1 year. Some major sewer lines collapsed in areas of permanent ground deformation. Loss of electric power affected pumping capacity and operations. Because of Higashinada Plant damage, sewage was released to Osaka Bay.</p>

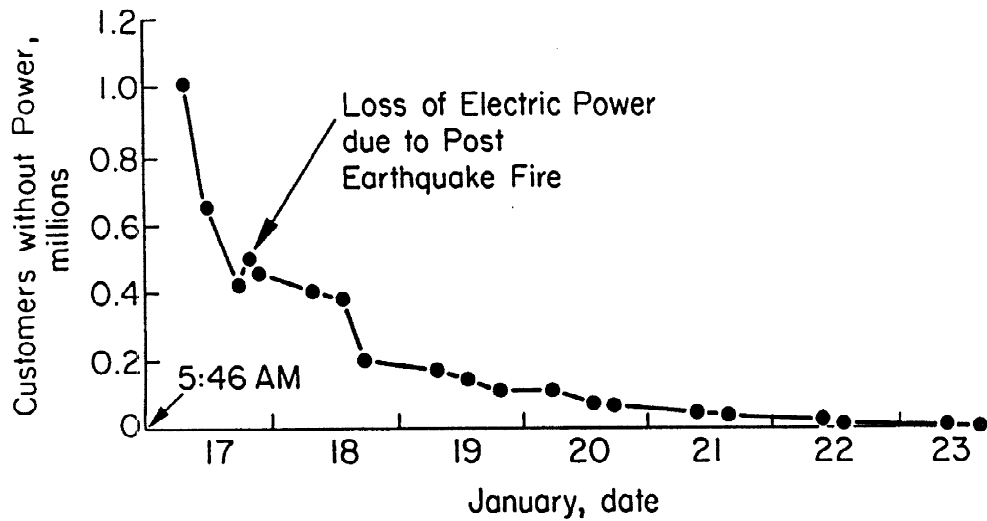


Fig. 1. Restoration of electric power after the 1995 Hyogoken-Nanbu earthquake

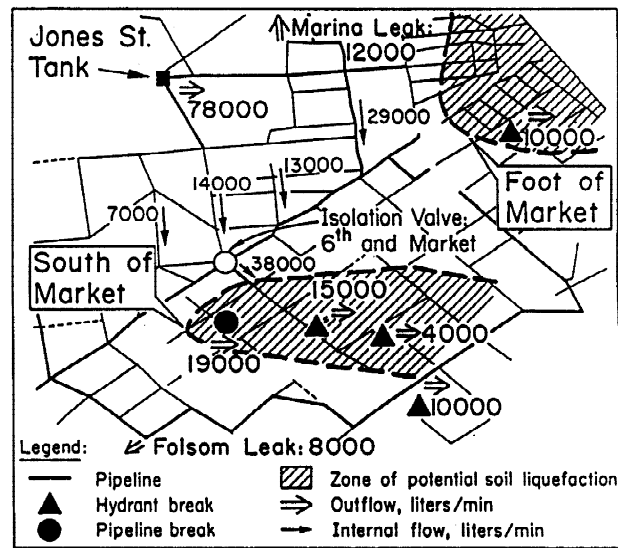
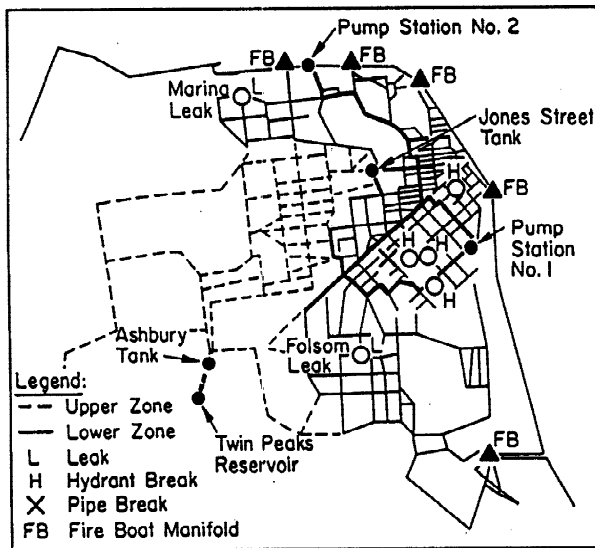


Fig. 2. AWSS damage after Loma Prieta earthquake (O'Rourke and Pease, 1992)

Fig. 3. Results of AWSS computer simulation (O'Rourke and Pease, 1992)

midway through the first day of the earthquake. This loss of power was caused by post earthquake fires that burned overhead electric lines and caused buildings to collapse on exposed distribution cables. Because electricity is an ignition source, the quick restoration of power in areas of leaking gas can cause additional fires.

In Kobe, electric power and natural gas facilities are operated by two independent companies. In contrast, electric power and natural gas in San Francisco are provided by the same company. Full restoration of electric power in San Francisco after the Loma Prieta earthquake took approximately two days while gas leak surveys were conducted.

Electric power affects remote control of the water supply, and thereby influences fire protection. As described by O'Rourke and Pease (1992), loss of water after the Loma Prieta earthquake was caused by pipeline breaks in response to liquefaction-induced ground movement. Water loss caused a critical reservoir, the Jones St. Tank, to empty, thereby leaving the Auxiliary Water Supply System (AWSS) in the central business district (CBD) of San Francisco without water.

Figure 2 shows a plan view of the AWSS that was simulated with a special computer program, GISALLE, to reproduce the conditions on the night of the earthquake. Water in the CBD was supplied by the Jones St. Tank. The lower and upper zones of the AWSS were isolated from one another with closed gate valves. Pump Stations 1 and 2 were not operated immediately after the earthquake, and were not included in the computer simulation.

Figure 3 shows analytical results in graphical format. Open arrows denote water egress either from the Jones St. Tank or damaged components. The solid arrows denote internal flow. The South of Market area had been recognized as a zone of potentially unstable ground, and had been isolated from adjoining portions of the network by closed gate valves. Only one open gate valve was provided for this zone at the intersection of Market and 6th Sts., as illustrated in the figure. This gate valve was designed to be operated remotely with utility-supplied electric power. Because of power loss, the valve could not be closed remotely. Consequently, water flow through this valve equals the sum of water losses from the broken main and two broken hydrants in this potentially unstable area of the system.

The total flow rate from the Jones St. Tank was approximately 78,000 liters/min. Given that the normal operating capacity of the Jones St. Tank is approximately 2.72 million liters of a maximum 2.84 million liters, the time required to empty the Jones St. Tank would have been about 35 minutes. This estimated time to loss of tank agrees with observations during the earthquake.

The failure of the remotely controlled isolation valve to be activated by utility-supplied electricity emphasizes the importance of identifying critical interfaces between lifeline systems and providing suitable backup for emergency conditions. The isolation valve now is connected to a battery pack that can be activated by radio.

Fire Following Earthquake

Fire following earthquake is a significant feature of each seismic event in Tables 1 and 2. Few people realize how close San Francisco came to a major conflagration after the 1989 Loma Prieta earthquake, even though the city operates the AWSS, which was constructed to provide an independent and supplemental network for major fires and earthquakes. As previously discussed, liquefaction-induced ground deformation broke pipelines which emptied an AWSS reservoir. At the same time, liquefaction-induced ground deformation heavily damaged the municipal water supply in the Marina. As a consequence, water was not available in either the AWSS or municipal system in the Marina when fire erupted there.

Fortunately, a Portable Water Supply System (PWSS) had been developed and organized before the earthquake. It consisted of vehicular hose tenders, each carrying about 1.5 km of 125-mm-diameter hosing and above ground hydrants. Three hose tenders were dispatched to the Marina, where they were able to contain and extinguish the fire, using water pumped from San Francisco Bay by the city's fireboat.

The conflagration after the 1995 Hyogoken-Nanbu earthquake invites comparisons with fires following the 1906 San Francisco and 1923 Kanto earthquakes. All three earthquakes resulted in extensive liquefaction with severe differential settlements and lateral displacements that ruptured buried water mains.

Figure 4 presents a bar graph showing the reservoir storage in San Francisco as a function of time after the 1906 earthquake. The amounts of water corresponding to Day 1 represent the quantities available roughly two hours after the earthquake struck. After four days, less than one-tenth of the initial capacity of the reservoir system, including the College Hill, University Mound, and Lake Honda Reservoirs, still was available. The system came dangerously close to complete failure, and large portions of the trunk line network were cut from the reservoirs by liquefaction-induced ground deformation. Fortunately, sufficient water was retained in the Lake Honda Reservoir to prevent fire spread across Van Ness Ave. into the western portions of the city. Fire following the 1906 earthquake remains the largest single fire loss in U.S. history, with approximately 11 km² burnt to the ground.

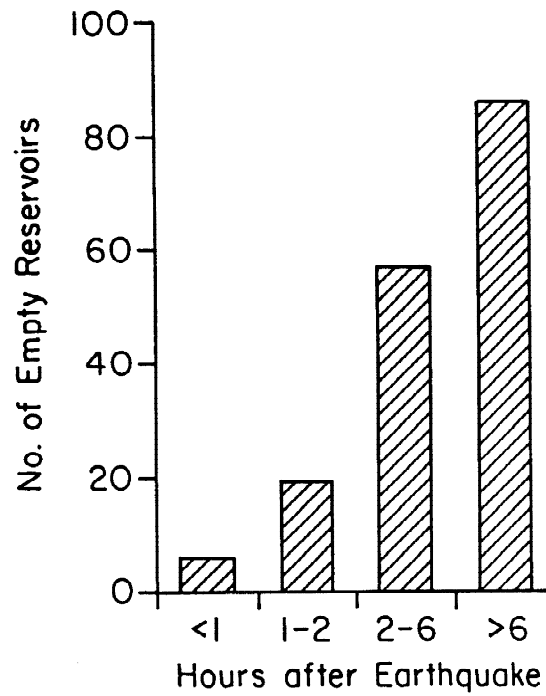
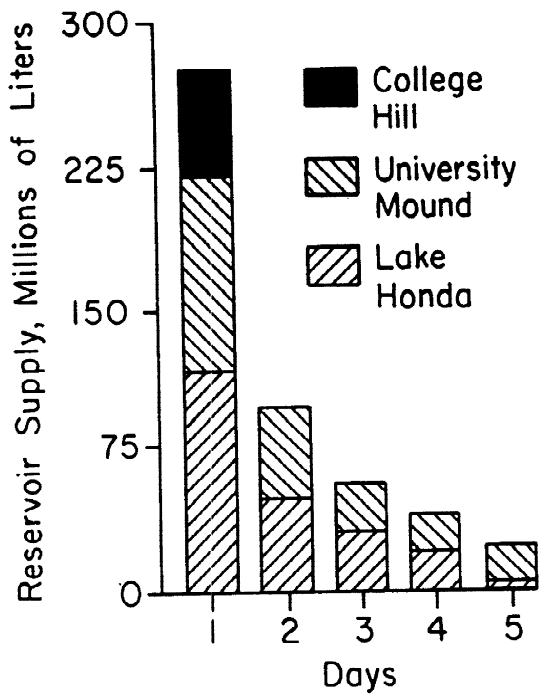


Fig. 4. Reservoir capacity after the 1906 San Francisco earthquake (O'Rourke and Pease, 1992)

Fig. 5. Loss of reservoirs after the 1995 Hyogoken-Nanbu earthquake

Figure 5 presents a bar chart of the number of Kobe reservoirs that emptied as a function of time after the 1995 Hyogoken-Nanbu earthquake. Like San Francisco, Kobe receives water by gravity flow from elevated reservoirs in the hills and mountains behind the city. Only one of the 86 reservoirs supplying Kobe was structurally damaged by the earthquake. All 86 reservoirs were empty within 24 hours after the main shock, primarily because of ruptures and disengagements of water pipelines. A significant amount of water was lost from pipelines damaged by liquefaction-induced ground movement. Perhaps a larger amount, however, was lost from thousands of broken services. Loss of water impaired fire fighting, with approximately 0.6 km² of Kobe City destroyed by fire.

As indicated in Table 1, there were 1610 repairs to distribution mains caused by the Hogoken-Nanbu earthquake, and 71,235 repairs in services, caused mostly by building damage. This pattern is similar to that of the 1906 San Francisco earthquake. O'Rourke, *et al.* (1992) have summarized the damage statistics compiled by the chief engineer of the 1906 San Francisco water supply, indicating 300 main breaks and 23,200 breaks in services caused by building damage. Although the number of main breaks is almost certainly an underestimate, the large number of services is similar in magnitude to the Kobe damage. Severe building damage, therefore, has an undesirable side effect of increasing water supply losses, with the potential for catastrophic water and fire losses in the event of a severe urban earthquake.

The events of the Loma Prieta earthquake show that flexibility provided in San Francisco by the PWSS was of critical importance in controlling and suppressing the fire that erupted in the Marina District. The ability to operate with portable hosing and draft from a variety of water sources, including underground cisterns and fireboats, provided a value extra dimension in the city's emergency response. Similar systems are recommended elsewhere for urban centers in seismically active areas.

Permanent Ground Deformation Effects

During earthquakes, permanent ground deformation can result from surface faulting, liquefaction, landslides, consolidation of granular soils, and tectonic uplift and subsidence. Because buried lifeline deformation is

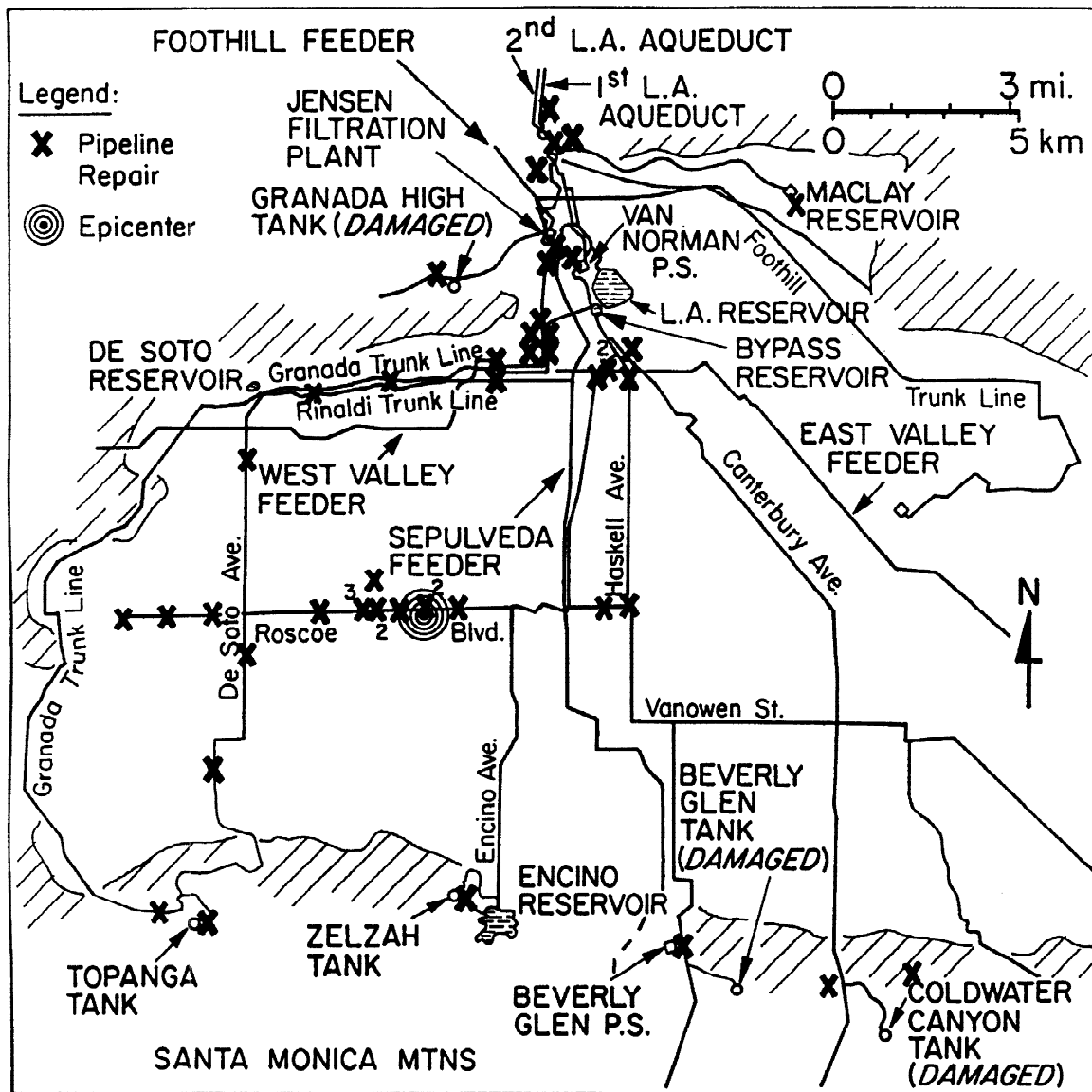


Fig. 6. Map of repair locations of water trunk lines after the 1994 Northridge earthquake

influenced strongly by soil movement, the fate of the ground is often the fate of the lifelines. Examples of damage to water supply, gas and liquid fuel, wastewater, and transportation facilities in Tables 1 and 2 show that geotechnical characteristics are critically important for most, if not all, lifeline systems. Permanent ground deformation effects on lifeline facilities has been the subject of substantial research and case history evaluation (e.g., Hamada and O'Rourke, 1992; O'Rourke and Hamada, 1992). Because of space limitations, further treatment of this subject is relegated to a forthcoming section in which protective coatings and wrappings to improve soil-pipeline interaction are discussed.

Lifeline Response to Transient Motion

The performance of buried lifelines in recent earthquakes, especially the 1994 Northridge earthquake, indicates that damage to buried transmission and trunk lines can be caused by transient motion, especially if the characteristics of the pipeline joints reduce axial compressive and tensile capacity. Figure 6 shows a plan view of selected repair locations to water trunk lines damaged by the Northridge earthquake in the San Fernando Valley. There were approximately 90 repairs to water trunk lines with diameters exceeding 300 to

600 mm. Most of the major trunk lines in the San Fernando Valley operated by the Los Angeles Department of Water and Power (DWP) and the Metropolitan Water District (MWD) sustained damage in at least one location. North of the area shown in the figure, there was damage in the two Los Angeles Aqueducts at 11 different locations, temporarily cutting supply from the reservoir system at Owen's Valley.

Repair statistics show damage in 67 steel trunk lines, with deformation or rupture recorded at approximately 34 welded slip joints. As described by Tawfik and O'Rourke (1985), a welded slip joint consists of a straight pipe end inserted into a flared or belled pipe end with a fillet weld applied circumferentially around the location where the pipe ends are mated. For pipe diameters less than about 1800 mm, the welds are applied externally. Tawfik and O'Rourke (1985) have shown that such joints have reduced capacity for axial compression. The pipelines, therefore, are vulnerable to permanent ground deformation. Given the special characteristics of near source motion generated by the Northridge earthquake, they are also susceptible to damage from transient motion. This subject is pursued further in the next section.

PIPELINE RESPONSE TO TRANSIENT MOTION

Transmission pipelines have been damaged in recent earthquakes by transient ground motion. When such damage is related to pipeline deterioration or the characteristics of older welds, it emphasizes the need to evaluate vulnerability according to factors, such as corrosion and past construction practices, which reduce capacity relative to that achieved with modern materials and procedures. When such damage occurs in pipelines built according to modern construction practices, it emphasizes the need to understand better the strong motion characteristics associated with the damage and to develop predictive tools to identify potentially vulnerable lines and troublesome sites.

Simplified procedures for analyzing pipeline response to seismic waves have been proposed by a variety of researchers (e.g., O'Rourke, *et al.*, 1985), and provide the basis for the simplified approach described in this work. Fig. 7a shows a plan view of a pipeline intersected by a sinusoidal wave, traveling at an azimuth of Ω with respect to the pipeline.

It is assumed that seismic excitation can be modeled as a traveling wave that retains constant shape as it crosses the pipeline. If the maximum longitudinal pipeline strain, ϵ_{pm} , equals the maximum ground strain, ϵ_{gm} , in the direction of the line, then:

$$\epsilon_{pm} = \epsilon_{gm} = \frac{v_p \cos^2 \Omega}{c} \quad (1)$$

in which v_p is the peak particle velocity in the direction of wave propagation and c is the wave propagation velocity. The maximum axial force in the pipeline is:

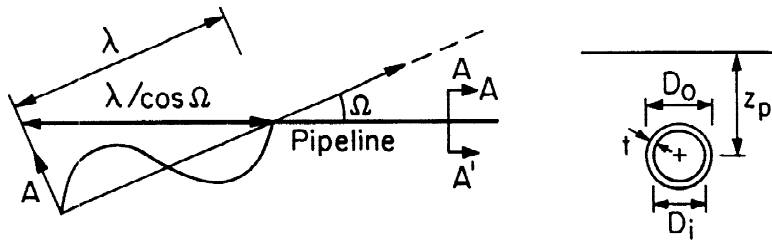
$$F_m = \frac{v_p \cos^2 \Omega EA}{c} \quad (2)$$

in which E is Young's modulus of the pipeline material and A is the cross-sectional area of the pipe.

One also needs to consider the frictional or adhesive force per unit length, f , conveyed to the pipe. With reference to Fig. 7b, the maximum pipe force, F_m , developed by shear transfer between pipeline and soil is:

$$F_m = \frac{f \lambda}{4 \cos \Omega} \quad (3)$$

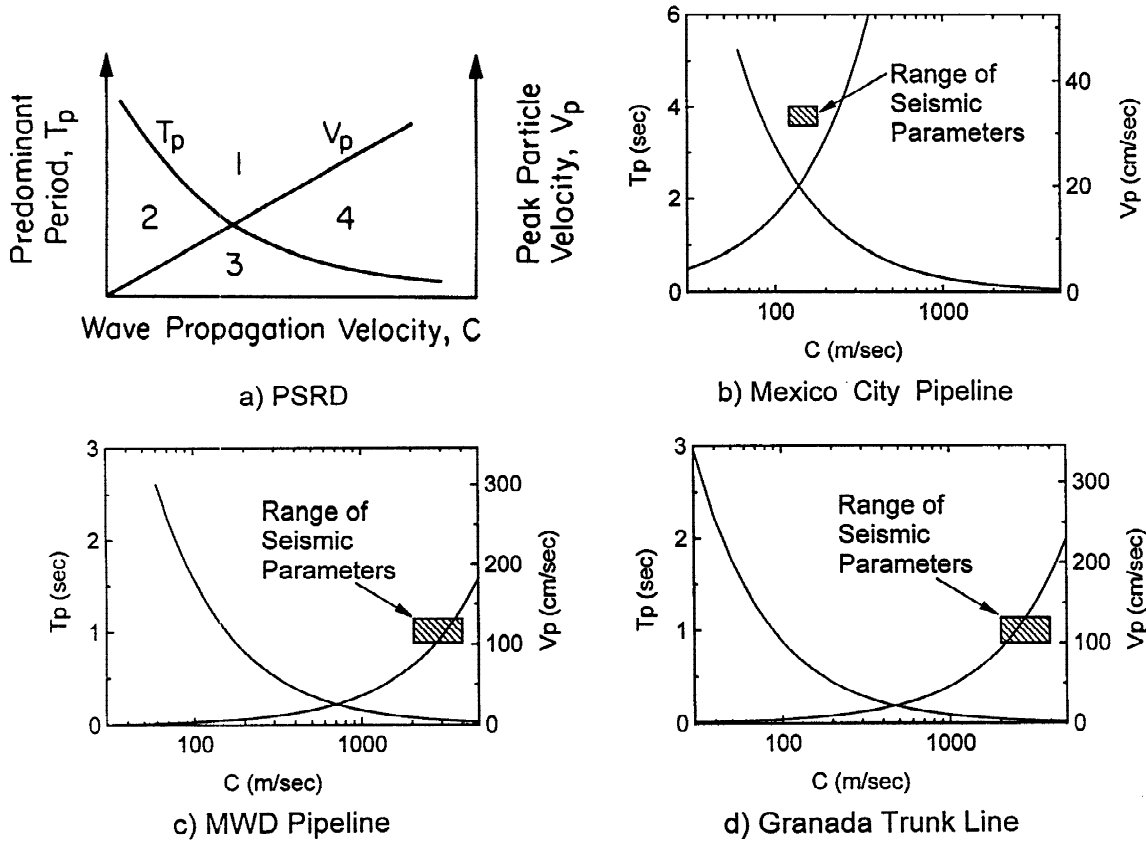
in which the frictional shear force per unit length, f , is given by:



a) Wave Orientation

b) Cross-section A-A'

Fig. 7. Seismic wave intersection with buried pipeline



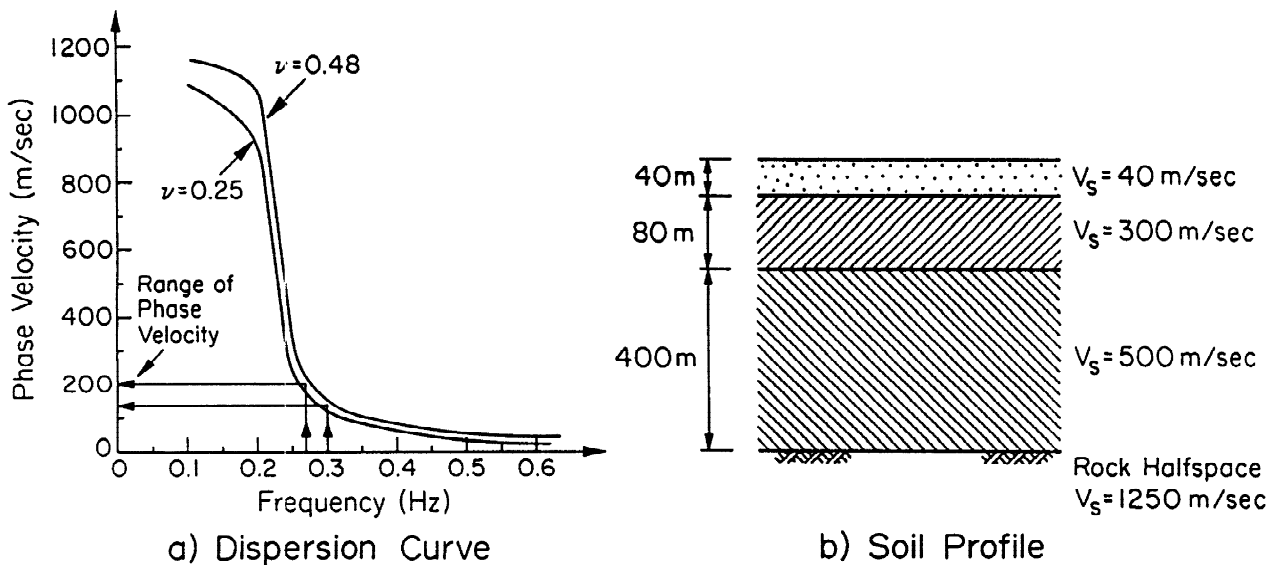
a) PSRD

b) Mexico City Pipeline

c) MWD Pipeline

d) Granada Trunk Line

Fig. 8. Pipeline seismic response diagrams



a) Dispersion Curve

b) Soil Profile

Fig. 9. R-wave dispersion curves and soil profile for Mexico City pipeline (Ayala and O'Rourke, 1989)

$$f = \left(\frac{1 + k_o}{2} \right) \gamma z_p \tan \delta \pi D_o \quad (4)$$

in which k_o is the at-rest lateral earth pressure coefficient (often assumed as $1 - \sin \phi' \leq k_o \leq 1.0$, where ϕ' = soil friction angle), γ is soil unit weight, z_p is the depth of the pipe center, δ is the friction angle between pipe and soil, and D_o is the outside pipe diameter. Recognizing that $\lambda = cT_p$:

$$F_m = \frac{f c T_p}{4 \cos \Omega} \quad (5)$$

If F_ℓ is the limit state force that causes failure or loss of serviceability, then Eqns. 2 and 5 can be rewritten to express the conditions in which the seismic wave characteristics exceed the pipeline limit state, namely:

$$v_p \geq \frac{F_\ell c}{E A \cos^2 \Omega} \quad (6)$$

$$T_p \geq \frac{4 F_\ell \cos \Omega}{f c} \quad (7)$$

Equations 6 and 7 indicate that the peak particle velocity and predominant period must exceed threshold values established by the limit state force, pipe properties, interface shear between pipe and soil, and wave propagation velocity to damage the pipeline. These conditions can be expressed conveniently in a pipeline seismic response diagram (PSRD), as illustrated in Fig. 8a where Eqns. 6 and 7 are plotted. The pipeline is vulnerable to damage only if the combination of T_p , v_p , and c plot in Zone 1. In Zone 2, v_p exceeds the limit conditions, but small c results in a wavelength insufficient to mobilize shear forces to exceed the limit state force. In Zone 4, the wavelength is of sufficient magnitude to mobilize the appropriate force, but v_p is too small to develop enough axial force to damage the pipe. Both T_p and v_p are below threshold values in Zone 4. The PSRD in Fig. 8a is based on analytical principles similar to those adopted by Ayala and O'Rourke (1989) to evaluate buried pipeline response to traveling ground waves during the 1985 Michoacan earthquake.

To test the simplified procedure relative to actual performance, PSRDs were developed for three pipelines. Fig. 8b shows the PSRD for the 1069-mm water transmission pipeline, damaged by transient motion during the 1985 Michoacan earthquake, described by Ayala and O'Rourke (1989). The pipeline was buried at a depth of 1.94 m in soil with $\gamma = 19.6 \text{ kN/m}^3$, $k_o = 1.0$ and $\delta = \phi' = 37^\circ$. The buckling capacity of the pipe was taken as approximately 290 MPa and the wall thickness was 7.9 mm. Values of v_p and T_p were assessed as 33 to 37 cm/s and 3.5 to 4 s, based on data provided by Ayala and O'Rourke, and it was assumed that $\Omega = 0$.

Figure 9 presents the R-wave dispersion curve and associated soil profile at the pipeline site. Strong motion data provided by Ayala and O'Rourke demonstrate a clear and consistent pattern of sinoisoidal waves in the area of interest with $T_p = 3.3$ to 4 s. For the corresponding frequencies of 0.3 and 0.25 Hz, Fig. 9 shows a phase velocity between 120 m/s and 200 m/s. The value of c was equated with the phase velocity.

Two trunk lines, which were damaged at welded slip joints, near the Jensen Treatment Plant during the 1994 Northridge earthquake also were evaluated with PSRDs. One line, which was operated by MWD, is 2160 mm in diameter, with 20.6-mm-thick wall, buried at 2.6-m depth in soil with $\gamma = 19.6 \text{ kN/m}^3$, $k_o = 1.0$, and $\delta = \phi' = 37^\circ$. The yield strength of the pipe is 249 MPa. No permanent ground deformation was reported at the location of damage. The other line is the Granada Trunk Line, operated by DWP. It is 1245 mm in diameter, with 6.4-mm-thick wall, buried at a 1.8-m depth in soil similar to that above. The yield strength of the pipe is 249 MPa. Although some portions of the pipeline were damaged by permanent ground deformation in this area, there is a relatively long distance where the pipeline is buried within the utility corridor adjacent to the Jensen Plant. This area was influenced by relatively small lateral movement

perpendicular to the line. Accordingly, some welded slip joint deformation in this area may have been caused by transient waves.

Both pipelines are oriented along the radial direction from the epicenter, and strong motion records obtained at the Jensen Plant and Sylmar Converter Station were resolved in this direction. Values of v_p were between 100 and 130 cm/s, c was estimated as 2 to 4 km/s, and T_p from the strong motion records was between 0.75 and 1.5 s. Because the pipelines are parallel to a radial path from the epicenter, Ω was taken as zero.

The limit state force for the pipelines was computed on the basis of the equations developed by Tawfik and O'Rourke (1985) for the compressive load capacity of welded slip joints. The failure mode proposed by Tawfik and O'Rourke is based on plastic deformation at the location of maximum curvature in the bell of the welded slip joint. Damage in the field occurred as wrinkling and cracking at this location of the bell.

As can be seen in Figs. 8b, c, and d, the seismic characteristics relevant for each pipeline plot in an area that overlaps with Zone 1 in Fig. 8a. The PSRDs, therefore, appear to provide a reasonable screening or estimation tool for identifying conditions in which transient motion can damage water trunk and transmission lines composed of steel.

There are two scenarios that apparently can promote traveling wave damage to steel water lines. At sites with deep soft soils, such as the one in Mexico City, surface waves tend to control damage. The combination of low wave propagation velocity and high predominant period can result in conditions where high ground strains develop in combination with relatively long wavelengths. In near source locations, such as the epicentral area of the Northridge earthquake, strong pulses of seismic excitation lead to predominant periods of approximately 1 s and high peak particle velocities. The high particle velocities result in ground strains of sufficient magnitude to generate high axial loads in the pipelines.

SEISMIC RESPONSE OF LIQUEFACTION SITES

Vertical array measurements at instrumented sites of liquefaction have shown relatively large transient shear strains in liquefied soils. O'Rourke and Pease (1995), for example, have summarized measurements interpreted from several vertical arrays to show maximum transient shear strains of approximately 1.5 to 2.0% in liquefied soil layers. When integrated over the thickness of liquefiable soil, transient lateral shear strains can have a strong influence on the lateral deformation imposed on buried pipelines.

Figure 10 from O'Rourke and Pease (1995) illustrates how buried pipelines are affected by ground deformation arising from settlement caused by post-liquefaction consolidation (Fig. 10b) and by lateral shear strains (Figs. 10c and d). As an approximation, surficial soil and pipeline lateral movements are equal to the product of the average lateral shear strain and the thickness of soil subjected to liquefaction. The magnitude of lateral displacement, therefore, will vary in direct proportion to the thickness of the liquefiable fill. Fig. 10d shows that lateral ground strains can result in axial compressive and tensile strains in a buried pipeline. If it is assumed that the pipeline deforms axially as the ground deforms (as would be appropriate for relatively thin wall pipe anchored in the ground by multiple service connections and tees), the maximum axial strain in the pipe, ϵ_a , is given by:

$$\epsilon_a = \Delta\delta_H / L \quad (8)$$

in which $\Delta\delta_H$ is the differential lateral displacement in the upper, non-liquefiable layer over a horizontal distance, L .

O'Rourke and Pease (1995) used a detailed three-dimensional model of subsurface conditions in the Marina of San Francisco, which was developed from over 250 borings and soundings, to evaluate the magnitudes and patterns of axial ground strains. They compared these strains with pipeline damage after the Loma Prieta earthquake. Maximum transient lateral shear strain in submerged fill at Treasure Island was estimated

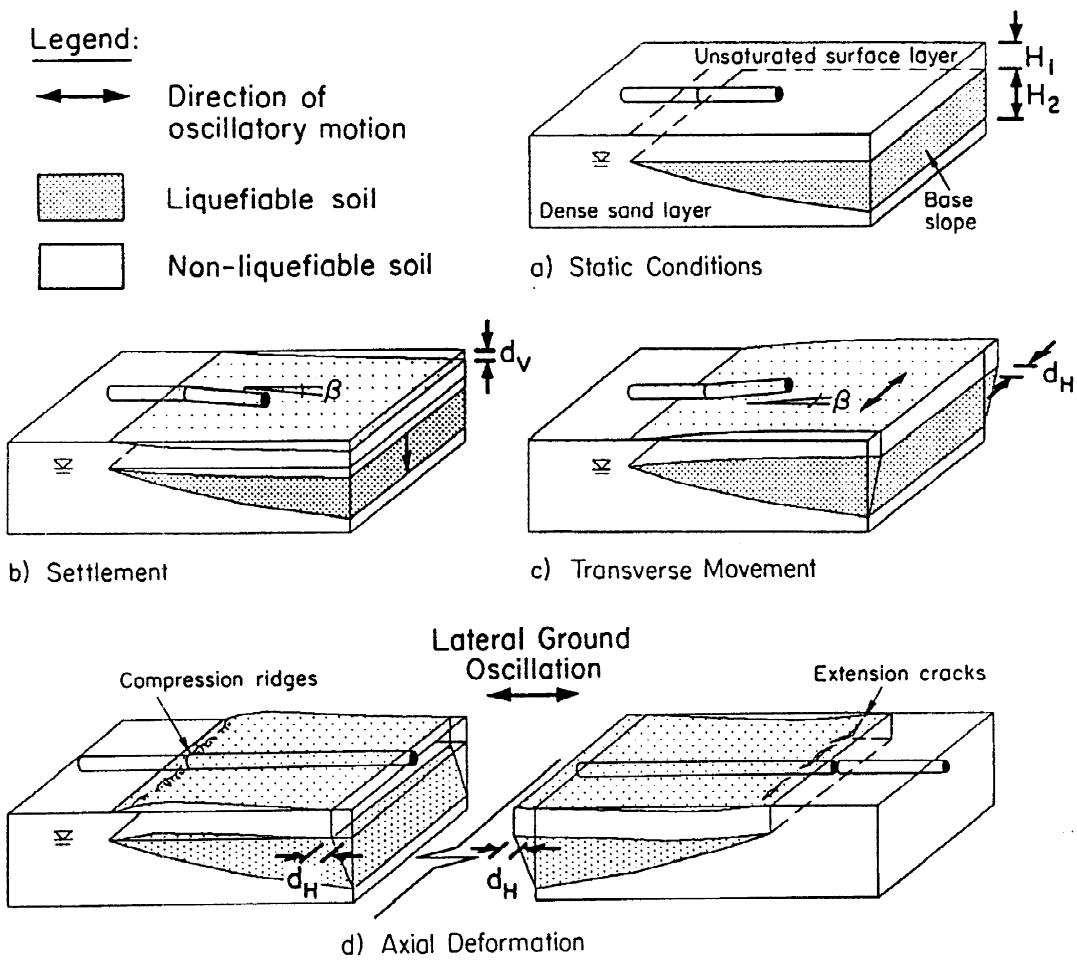


Fig. 10. Schematic of buried pipeline response to transient displacements at a liquefaction site (O'Rourke and Pease, 1995)

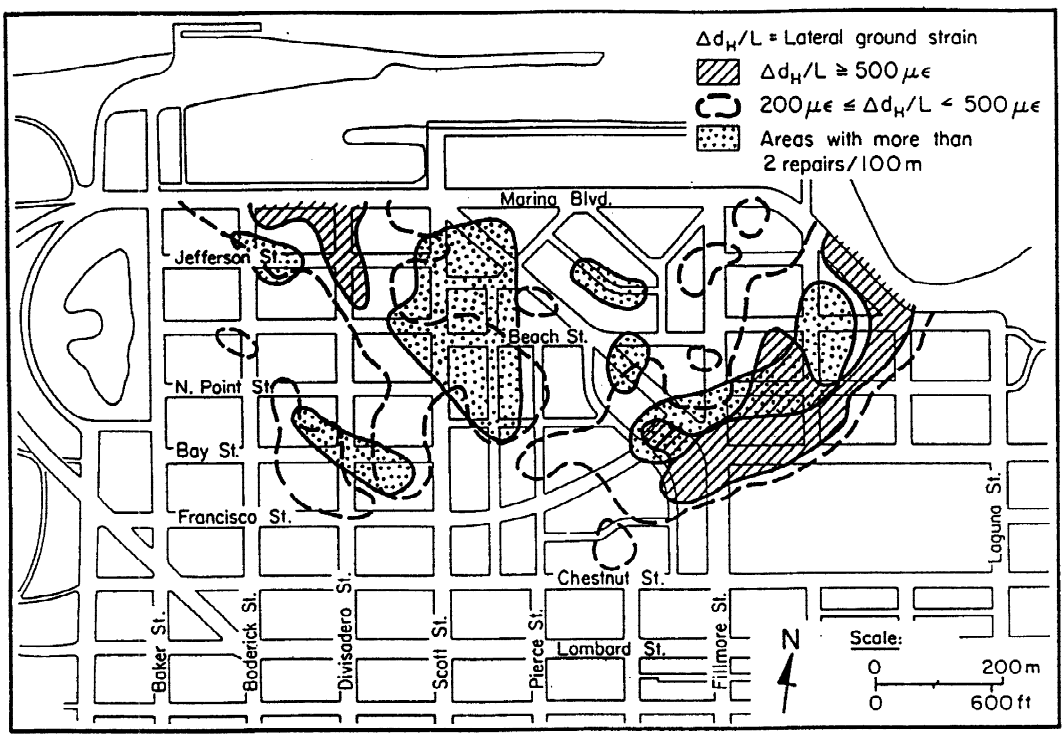


Fig. 11. Comparison of axial strains and pipeline damage in the Marina (O'Rourke and Pease, 1995)

from strong motion records as approximately 2% in the east-west direction, which corresponds to the azimuth of strongest recorded ground acceleration. Similarly, a lateral shear strain of 1.25% in the north-south direction was estimated from a ratio of 1.6 between east-west and north-south components of maximum ground motion. Using these strains at the Marina, in conjunction with the submerged fill thickness from the three-dimensional subsurface model, computer analyses were used to determine lateral displacement patterns for both the north-south and east-west alignments. Taking the first derivatives of these functions at various locations, the maximum lateral ground strains affecting north-south and east-west oriented pipelines were calculated to delineate zones of maximum lateral strain affecting buried pipelines in Fig. 11. These zones are compared with areas which experienced the highest concentrations of pipeline damage of more than 2 repairs/100 m.

Of particular significance is that lateral ground strains varying from 200 to 900 $\mu\epsilon$ are predicted over a significant portion of the submerged fill. These levels of strain are fully compatible with levels sufficient to damage cast iron pipelines. There is reasonably good agreement between the areas of maximum lateral ground strain in Fig. 11 and those with the highest concentration of pipeline damage. In particular, there is close agreement along the southeastern and western margins of the fill.

Although pipeline damage correlates well with locations of maximum lateral ground strain, it should be recognized that the actual causes of pipeline damage are related to complex interactions. O'Rourke and Pease (1995) point out that, rather than viewing lateral ground strain as a cause of axial failure, it is more appropriate to regard strain as an index of local deformation imposed during the earthquake.

The field data and analytical assessments developed for the Marina pipeline system are highly significant because they show for the first time how transient horizontal deformation at liquefaction sites affects the performance of buried utilities. They also show how the three-dimensional characteristics of liquefiable soils control the pattern of transient lateral displacements at the ground surface.

Mapping the thickness of liquefiable deposits provides an excellent means of locating areas of potentially severe liquefaction and showing their relationship with underground utilities, buildings, and transportation facilities. It is well known that the thickness of liquefiable fill influences the magnitude of lateral spread and surface settlement caused by liquefaction. The more recent findings show that liquefaction also affects transient motions, potentially resulting in large axial strains. The thickness of a liquefiable fill or natural sand deposit is easily adapted to Geographical Information Systems (GIS), and thus can provide an effective vehicle for assessing urban hazards, microzoning for seismic hazard reduction, and planning for optimal lifeline performance during an earthquake.

SOIL-PIPELINE INTERACTION

Figure 12 shows a pipeline subjected to abrupt soil displacement that could occur at a fault crossing or along the margins of a landslide. The distance between the fault and anchor point is known as the anchor length, L_a . Anchors may be caused by bends, tie-ins, and other features that develop substantial resistance to axial movement. Alternatively, the anchor point may represent an effective anchor length, beyond which there is no axial stress imposed in the pipeline from the abrupt ground movement. It has been noted by several researchers (e.g., Newmark and Hall, 1975; Kennedy, *et al.*, 1977) that the maximum axial strain imposed in the pipe at a fault crossing is inversely related to anchor length. Long anchor lengths will reduce axial strain, and can be developed by reducing the frictional or adhesive force per unit length of pipeline, f .

Pipeline wrap and coatings have a strong influence on the shear forces conveyed from soil to pipe. The values of f (see Eqn. 4) associated with different pipeline coatings will depend on the roughness and hardness of the pipe/soil interface. For rough interfaces, such as those of cement-coated water trunk lines, shear failure is displaced into the soil immediately adjacent to the interface. The angle of interface friction, δ , therefore, is equal to the friction angle of the soil, ϕ' . As the interface becomes progressively smoother and harder, the value of δ declines to a fraction of ϕ' . Table 3 summarizes values of δ/ϕ' appropriate for various coatings. It should be noted that a coating, such as coal tar epoxy, is relatively soft so that soil

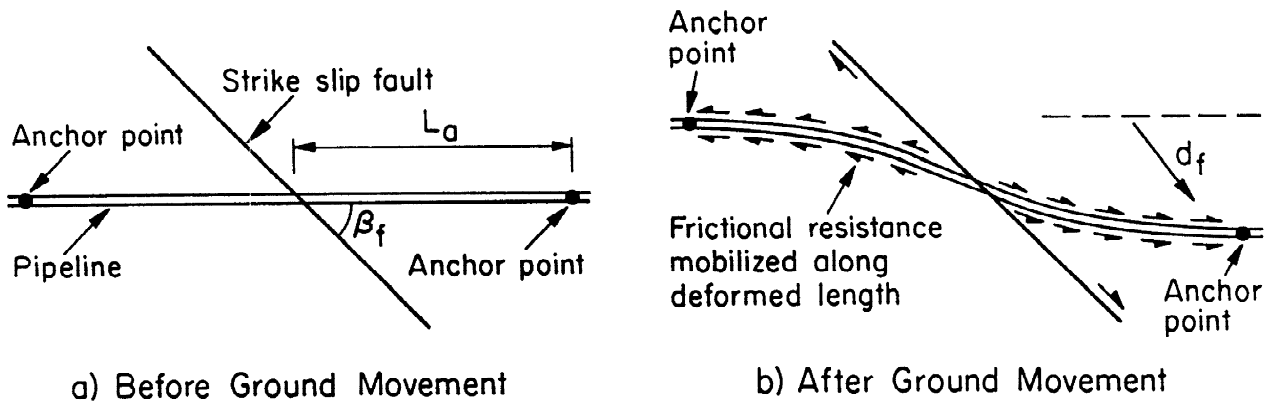


Fig. 12. Axial pipeline-soil interaction near abrupt ground movement

Table 3. Pipeline interface angles of friction for contact with granular soil

Pipeline interface material	Ratio of interface to soil angle of friction, $\delta\phi$, or δ -value for design
Rusted and pitted steel, partially cemented and bonded to adjacent soil; rough concrete and cement coatings	1.0
Soft coatings and wrappings, such as coal tar enamels, hot or cold applied mastics, and coal tar epoxies	$\delta = 30^\circ$
Rough steel, some oxidation and rusting of surface with minor pitting; smooth, finished concrete surface	0.7 - 0.9
Resin epoxy coating ^a	0.6 - 0.8
Polyolefin or polyethylene coating	0.6 - 0.7
“Frictionless” wrap, employing geogrid on polyethylene, polyolefin, or epoxy coating (see Fig. 13)	$\delta = 10^\circ\text{-}15^\circ\text{b}$

a - Assumes some aging and softening

b - Based on lab tests (Mitchell, *et al.*, 1990) and full scale field tests (Trigg, 1995)

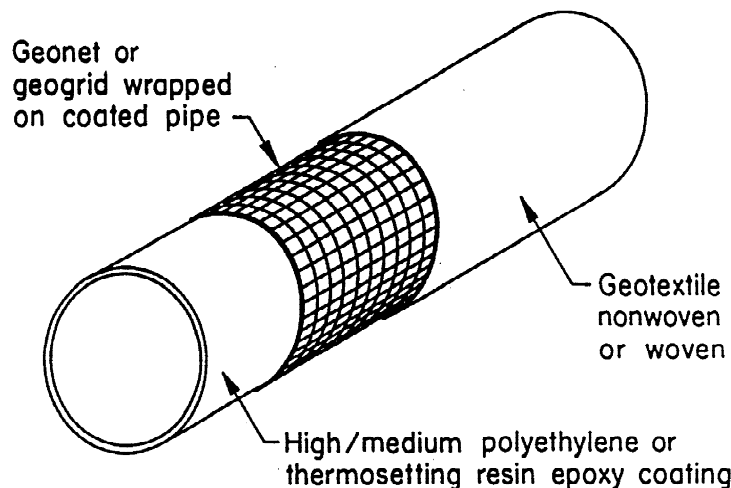


Fig. 13. “Frictionless” pipeline wrap for landslide and active fault zones (Patent pending through Cornell University)

grains become embedded in the coating, thereby increasing its frictional resistance. O'Rourke, *et al.* (1990) showed that the limiting condition of δ for soft coatings is equivalent to the critical void ratio angle of shearing resistance, ϕ'_{cv} , where $\tan \delta = \sin \phi'_{cv}$. For most soft coatings the interface frictional resistance can be estimated from $\delta = 30^\circ$. Research results show that a polymer coating with Shore D Hardness ≤ 45 qualifies as a soft coating.

Inspection of Table 3 reveals that the lowest $\delta\phi'$ is generated by polyethylene, polyolefin, and fusion-bonded resin epoxies. In principle, it is possible to reduce the interface friction to very low values, equivalent to $\delta\phi'$ of about 0.25 by providing for a sliding surface between a polyethylene sheet and polyethylene grid. Laboratory tests of these types of interfaces show extremely low friction (Mitchell, *et al.*, 1990).

Figure 13 shows a three-dimensional view of a pipe wrap that promotes minimal shear transfer from soil to pipe. The wrap creates a low friction sliding interface between the epoxy or polyethylene coating of the pipe and a geonet or geogrid. Geonets and geogrids are polymer meshes available commercially for subsurface drainage and soil reinforcement, respectively. Intrusion of soil into the open spaces of the geonet or geogrid is prevented by a geotextile which surrounds the pipe. The geotextile may be either woven or non-woven. The geotextile also provides a porous covering so that soil moisture can penetrate the wrapping. The porous nature of the covering is essential for cathodic protection because it allows electrolyte penetration, thus permitting electric current to be impressed on the pipeline. The geogrids, geonets, and geotextiles used in the wrap are relatively inexpensive and readily available. Moreover, the wrap can be applied in the field easily, with minimal time delay, and located as required along all or selected lengths of the pipeline.

The "frictionless" wrap has been evaluated by full-scale pullout tests on 400-mm pipe performed by NOVA Gas Transmission, Ltd. (Trigg, 1995). The wrap was found to reduce longitudinal shear forces to approximately one-third of those for unwrapped pipe. It is intended to use the wrap in landslide areas to reduce longitudinal forces conveyed to pipelines by soil displacements.

GIS AND REAL TIME MONITORING

A hydraulic network model, such as that performed for the San Francisco AWSS (see Fig. 3), not only provides for a graphical assessment of system performance, but allows for coordinated management and improvement of lifeline systems when linked to GIS. Ayala (1996) and coworkers, for example, have used GIS to represent the water trunk and distribution system for Mexico City, and have combined this representation with databases on soil conditions and seismic parameters. Similar GIS modeling has been described by Shinozuka, *et al.* (1993) and various researchers worldwide. When analytical tools, such as hydraulic network analyses, are combined with GIS, earthquake damage states can be assessed on a probabilistic basis for planning new construction, retrofit, and emergency services.

Eguchi, *et al.* (1995) report on how rapid damage assessment tools, based on GIS, were used to facilitate response and recovery decisions after the Northridge earthquake. Data from near real-time broadcasts of earthquake source information were combined with computer models for loss estimation to evaluate probable scenarios of damage and recovery. Techniques are being developed to use satellite data and air photo reconnaissance to compare estimated damage levels with post-earthquake effects.

Because of space limitations, it is not possible here to do justice to this important topic. It is probable, however, that reviews of lifeline engineering in forthcoming world conferences will focus on computer-based management and modeling. Because of the diversity and geographical coverage associated with lifelines, it is inevitable that GIS-assisted modeling will become increasingly more important for engineering and planning. Only by graphically interlaying databases for seismic, geotechnical, economic, social, and lifeline characteristics can the full complexity of this combination of factors be represented in a way which preserves space- and time-dimensional relationships. Future research and development efforts will concentrate on data acquisition, probabilistic analyses, and simplification of complex interactions to improve accuracy, communication, and decision making for lifeline systems.

ACKNOWLEDGMENTS

The preparation of this paper and much of the research reported herein was supported by the National Center for Earthquake Engineering Research, Buffalo, NY. The author is most grateful for the assistance of Mr. S. Toprak, who helped with the analyses of pipeline response to transient motion, and Professor A.G. Ayala, who reviewed the manuscript. Ms. L. McCall typed the manuscript, and Mr. A. Avcişoy prepared the figures.

REFERENCES

- Ayala, A.G. and M.J. O'Rourke (1989). Effects of the 1985 Michoacan earthquake on water systems in Mexico. *NCEER-89-0009*, National Center for Earthquake Engineering Research, Buffalo, NY.
- Ayala, A.G. (1996). Personal communication.
- EERI (1990). Loma Prieta earthquake reconnaissance report. *Earthquake Spectra, Supplement to Vol. 6*, Earthquake Engineering Research Institute, Oakland, CA.
- EERI (1995). Northridge earthquake of January 17, 1994 reconnaissance report. *Supplement C to Vol. 11*, Earthquake Engineering Research Institute, Oakland, CA.
- Eguchi, R.T. and H.A. Seligson (1995). Rapid post-earthquake damage assessment for lifeline facilities. paper presented at *6th US-Japan Workshop on Earthquake Disaster Prevention for Lifeline Systems*, Osaka, Japan, 12 p.
- Hamada, M. and T.D. O'Rourke, Eds. (1992). Case studies of liquefaction and lifeline performance during past earthquakes. *NCEER-92-0001, Vol. 1*, National Center for Earthquake Engineering Research, Buffalo, NY.
- Kennedy, R.P., A.W. Chow, and R.A. Williamson (1977). Fault movement effects on buried oil pipeline. *J. of the Transportation Engineering Division, Vol. 103, No. TE5*, ASCE, New York, NY, 617-633.
- McNutt, S.R. (1990). Summary of damage and losses caused by the Loma Prieta earthquake. *Special Publication 104*, California Division of Mines and Geology, Sacramento, CA, 131-138.
- Mitchell, J.K., R.B. Seed, and H.B. Seed (1990). Kettleman Hills waste landfill slope failure I: liner-system properties. *J. of Geotechnical Engineering, Vol. 116, No. 4*, ASCE, New York, NY, 647-669.
- Newmark, N.M. and W.J. Hall (1975). Pipeline design to resist large fault displacement. *Paper UILU-ENG-75-2011*, presented at the US National Conference on Earthquake Engineering, Ann Arbor, MI, 416-425.
- NIST (1996). The January 17, 1995 Hyogoken-Nanbu (Kobe) earthquake. *National Institute of Standards and Technology* (R.M. Chung, Ed.), Bethesda, MD.
- NRC (1994). Practical lessons learned from the Loma Prieta earthquake. *National Research Council*, National Academy Press, Washington, DC.
- O'Rourke, T.D., M.D. Grigoriu, and M.M. Khater (1985). Seismic response of buried pipes. *Pressure Vessel and Piping Technology - A Decade of Progress* (C. Sundararajan, Ed.), ASME, New York, NY, 281-323.
- O'Rourke, T.D., S.J. Druschel, and A.N. Netravali (1990). Shear strength characteristics of sand-polymer interfaces. *J. of Geotechnical Engineering, Vol. 116, No. 3*, ASCE, New York, NY, 451-469.

- O'Rourke, T.D., P.A. Beaujon, and C.R. Scawthorn (1992). Large ground deformations and their effects on lifeline facilities: 1906 San Francisco earthquake. *Case Studies of Liquefaction and Lifeline Performance During Past Earthquakes* (T.D. O'Rourke and M. Hamada, Eds.), *NCEER-92-0002*, National Center for Earthquake Engineering Research, Buffalo, NY, 1-1 - 1-130.
- O'Rourke, T.D. and M. Hamada, Eds. (1992). Case studies of liquefaction and lifeline performance during past earthquakes. *NCEER-92-0002, Vol. 2*, National Center for Earthquake Engineering Research, Buffalo, NY.
- O'Rourke, T.D. and J.W. Pease (1992). Large ground deformations and their effects on lifeline facilities: 1989 Loma Prieta earthquake. *Case Studies of Liquefaction and Lifeline Performance During Past Earthquakes* (T.D. O'Rourke and M. Hamada, Eds.), *NCEER-92-0002*, National Center for Earthquake Engineering Research, Buffalo, NY, 5-1 - 5-85.
- O'Rourke, T.D. and J.W. Pease (1995). Lessons learned from liquefaction and lifeline performance during San Francisco earthquakes. *Proceedings, Vol. 2*, Third International Conference on Recent Advances in Geotechnical Earthquake Engineering and Soil Dynamics, St. Louis, MO, 1017-1037.
- Schiff, A., Ed. (1995). Northridge earthquake lifeline performance and post-earthquake response. *TCLÉE Monograph No. 8*, Am. Soc. of Civil Eng., New York, NY.
- Shinozuka, M., H. Hwang, and S. Tanaka (1993). GIS-based assessment of the seismic performance of a water delivery system. *Proceedings, Fifth US-Japan Workshop on Earthquake Disaster Prevention for Lifeline Systems* (K. Kawashima, H. Sugita, and T. Nakajima, Eds.), *PWRI 3198*, Public Works Research Institute, Tsukuba, Japan, 233-249.
- Shinozuka, M., Ed. (1995). The Hanshin-Awaji Earthquake of January 17, 1995 Performance of Lifelines. *NCEER-95-0015*, National Center for Earthquake Engineering Research, Buffalo, NY.
- Tawfik, M.S. and T.D. O'Rourke (1985). Load-carrying capacity of welded slip joints. *J. of Pressure Vessel Technology, Vol. 107, No. 1*, ASME, 36-43.
- Trigg, A. (1995). "Frictionless" pipe wrap test results - ASC pipe/soil interaction test centre. NOVA Gas Transmission, Ltd., Calgary, Alberta, Canada.
- UNCRD (1995). Comprehensive Study of the Great Hanshin Earthquake. *Research Report Series 12*, United Nations Centre for Regional Development, Nagoya, Japan.